© 2022. Published by The Company of Biologists Ltd | Development (2022) 149, dev200159. doi:10.1242/dev.200159

RESEARCH ARTICLE

Engrailed, Suppressor of fused and Roadkill modulate the *Drosophila* GLI transcription factor Cubitus interruptus at multiple levels

Nicole Roberto[1], Isabelle Becam[2], Anne Plessis[2] and Robert A. Holmgren[1,*]

ABSTRACT

Morphogen gradients need to be robust, but may also need to be tailored for specific tissues. Often this type of regulation is carried out by negative regulators and negative feedback loops. In the Hedgehog (Hh) pathway, activation of *patched* (*ptc*) in response to Hh is part of a negative feedback loop limiting the range of the Hh morphogen. Here, we show that in the *Drosophila* wing imaginal disc two other known Hh targets genes feed back to modulate Hh signaling. First, anterior expression of the transcriptional repressor Engrailed modifies the Hh gradient by attenuating the expression of the Hh pathway transcription factor *cubitus interruptus* (*ci*), leading to lower levels of *ptc* expression. Second, the E-3 ligase Roadkill shifts the competition between the full-length activator and truncated repressor forms of Ci by preferentially targeting full-length Ci for degradation. Finally, we provide evidence that Suppressor of fused, a negative regulator of Hh signaling, has an unexpected positive role, specifically protecting full-length Ci but not the Ci repressor from Roadkill.

KEY WORDS: Hedgehog, Signal transduction, Pathway modulation, *Drosophila*

INTRODUCTION

The Hedgehog (Hh) pathway is one of a small number of signaling cascades essential for the proper development of most animals. It plays a key role in patterning arthropod segments and numerous tissues in mammals (Lee et al., 2016). Defects in Hh signaling lead to a number of congenital abnormalities including holoprosencephaly, whereas inappropriate activation of the pathway is involved in several important human cancers including basal cell carcinoma and medulloblastoma (Briscoe and Thérond, 2013).

Hh reception and early transduction involves several transmembrane proteins, including its co-receptor Patched (Ptc) and the G Protein Coupled Receptor (GPCR) Smoothened (Smo). In the absence of Hh, Ptc negatively controls Smo, likely by controlling its access to accessible cholesterol (Radhakrishnan et al., 2020; Kinnebrew et al., 2021), leading to the internalization and degradation of Smo. Binding of Hh to Ptc, however, relieves Ptc repression of Smo (Taipale et al., 2002) and promotes its hyperphosphorylation by multiple kinases (Chen and Jiang, 2013). Activated Smo recruits a complex composed of Costal2 (Cos2; also known as Cos), the Fused (Fu) kinase and Cubitus interruptus (Ci) (Robbins et al., 1997; Sisson et al., 1997). Activation of the Fu kinase is required for high level Hh signaling (Alves et al., 1998; Zhou et al., 2006; Ranieri et al., 2012; Sanial et al., 2017; Giordano et al., 2018; Han et al., 2019) and the release of Ci for translocation into the nucleus (Lefers et al., 2001).

As in other signaling systems, the Hh pathway is subject to a number of regulatory loops to ensure that it is activated in the appropriate locations and that responses are robust and precise. One of the best known feedback loops is that involving *ptc*. The *ptc* gene is a transcriptional target of Hh signal transduction, and its activation by Hh signaling leads to increased sequestration and degradation of Hh, limiting its range of action (Chen and Struhl, 1996). Another feedback loop that acts positively involves the interplay between Smo and the Fu kinase (Claret et al., 2007; Sanial et al., 2017).

A second level of regulation is the processing of the Ci transcription factor into a repressor in the absence of Hh signaling (Aza-Blanc et al., 1997). The production of the Ci repressor ensures that Hh target genes are actively repressed in the absence of signal and generates a reciprocal gradient to that of the full-length Ci transcriptional activator (Parker et al., 2011). A surprising consequence of these reciprocal gradients is that genes such as *ptc* that contain enhancers with consensus Ci binding sites are only expressed in response to high level Hh signaling, whereas genes such as *decapentaplegic* (*dpp*) that contain enhancers with imperfect Ci binding sites are expressed in response to modest level Hh signaling. Parker et al. (2011) demonstrated that replacing the imperfect Ci binding sites in a *dpp* enhancer with perfect Ci binding sites caused the expression of this enhancer to shift from the domain of modest level Hh signaling to the domain of high level Hh signaling along the compartment boundary. The authors concluded that the Ci repressor was able to outcompete the full-length Ci activator form for binding to these perfect sites.

To explore other potential feedback loops involving Hh target genes, we examined the roles of the transcription factor *engrailed* (*en*) in Hh signaling. It was originally thought that, in *Drosophila*, expression of *en* defines the posterior compartment where Hh is produced and is required *for hh* expression (Tabata et al., 1992), whereas expression of *ci* defines the anterior compartment (Hh-receiving cells). In the wing disc pouch, the *en* gene is also activated in the anterior compartment of the wing pouch in response to the highest levels of Hh signaling (Blair, 1992). The role of this anterior expression of *en* is not well understood, though it does downregulate the expression of *dpp* (Strigini and Cohen, 1997), and its region of expression corresponds to that identified as a region currently considered to contain a labile high-activity form of Ci (Ohlmeyer and Kalderon, 1998). Here, we show that anterior expression of *en*

[1]Department of Molecular Biosciences, Northwestern University, Evanston, IL 60201, USA. [2]Université de Paris, CNRS, Institut Jacques Monod, F-75013 Paris, France.

*Author for correspondence (r-holmgren@northwestern.edu)

R.A.H., 0000-0002-8638-0459

Handling Editor: James Briscoe
Received 1 September 2021; Accepted 3 February 2022

Development (2022) 149, dev200159. doi:10.1242/dev.200159

attenuates the expression of *ci*, leading to decreased levels of *ptc* expression. This modifies the Hh gradient and results in an expansion of the domain between longitudinal wing veins three and four.

We also examine the role of a second Hh target gene, *roadkill* (*rdx*) (also known as *hib*). *rdx* was identified as a gene activated in response to Hh signaling. *rdx* encodes an E-3 ligase that functions with Cul3 to target proteins for degradation by the proteasome (Kent et al., 2006; Zhang et al., 2006). Unlike Slmb and Cul1, which mediate Ci processing into the repressor, Rdx causes the complete degradation of Ci from both the N and C termini (Zhang et al., 2009). Rdx has also been implicated in regulating the nuclear import of Ci (Seong et al., 2010). In overexpression experiments, it has been shown that the Ci-interacting protein Suppressor of fused [Su(fu)] competes with Rdx for binding to Ci and partially protects Ci from Rdx-mediated degradation (Zhang et al., 2006) and regulates this process *in vivo* (Seong and Ishii, 2013). Notably, Rdx plays an important role in the degradation of Ci posterior to the morphogenetic furrow in the eye disc, where loss of *rdx* leads to a disruption in ommatidial packing (Kent et al., 2006; Zhang et al., 2006). The eye disc is unique in that the domain between Hh signaling and Hh receiving cells shifts with the movement of the morphogenetic furrow (Strutt and Mlodzik, 1997). As a consequence, cells must rapidly transition from expressing high levels of Ci to shutting off its expression.

Here, by engineering competition between full-length Ci and a truncated repressor-like form of Ci, Ci^{Ce2}, we show that Rdx preferentially targets full-length Ci. Moreover, we demonstrate that Su(fu) specifically protects full-length Ci from nuclear-localized Rdx (Zhang et al., 2006; Seong and Ishii, 2013; Liu et al., 2014), allowing it to successfully compete with Ci^{Ce2}. This reveals an as yet undescribed positive role for Su(fu). Together, our data reveal previously unreported regulatory processes that control Hh signaling via finely tuning Ci levels and activity.

RESULTS

Anterior *en* expression attenuates *ci* expression, extending the range of Hh signaling

In the *Drosophila* wing, the domain between longitudinal wing veins three (LV3) and four (LV4) is directly patterned by Hh signaling (Strigini and Cohen, 1997) and the location of the third wing vein primordium is determined by the range of Hh signaling (Biehs et al., 1998). This signaling process needs to be accurately regulated as the positioning of the third wing vein is precise to within one cell diameter (Abouchar et al., 2014).

To examine the role of anterior *en* expression on wing morphogenesis, we used a *ptc-GAL4* driver to express two *UAS-RNAi* constructs targeting *en* and *invected* (*inv*) (*inv* is an inverted gene duplication of *en*) in the region of the anterior compartment adjacent to the compartment boundary (Fig. 1). As can be seen in Fig. 1C, the distance between LV3 and 4 is significantly reduced in animals in which the expression of *en* and *inv* has been attenuated in the cells of the anterior compartment that abut the anterior/posterior (A/P) boundary. A corresponding posterior shift in the position of the third wing vein primordium is also observed in the developing wing disc using antibodies to the Blistered (Bs) protein, which marks cells destined to make the intervein region (Fig. 2A1-A3,B1-B3,C,D). We also observed an analogous shift in the domain of *dpp* expression (Fig. 2A2,B2,C,D).

A decrease in the distance between LV3 and LV4 is generally considered to be a consequence of a reduced Hh gradient or to decreased Hh signaling. To test whether Hh signaling had been altered, clones mutant for en^{E}, a deletion mutation that removes both the *en* and *inv* genes, were generated, and the expression of *ptc* assayed. Surprisingly, the expression of *ptc-lacZ* is increased in clones mutant for en^{E} (Fig. 3A,B). *ptc* expression depends on Ci, and we also observed elevated levels of full-length Ci protein in the *en* mutant clones that are directly adjacent to the compartment boundary (Fig. 3A,B). This effect is associated with an increase in the expression of a transcriptional reporter of *ci*, ci^{Dplac} (Fig. 3C,D). Moreover, the domain of attenuated Ci corresponds precisely with the domain of anterior *en* expression, and shifts with it when *en* expression expands in response to activated Smo and is eliminated when Smo function is attenuated (Fig. S1).

Anterior expression of *en* is not observed in early third instar larvae but becomes prominent by late third instar (Blair, 1992). To examine the consequences of this temporal change in anterior *en* expression, we used a dual-color fluorescent transcriptional timer, *UAS-TransTimer* (*UAS-TT*) (He et al., 2019). In this system, a *GAL4 UAS* controls the expression of a bicistronic message encoding a destabilized GFP (half-life ∼2.1 h) followed by RFP (half-life ∼18.5 h). We assessed the dynamics of *ci* expression by using *ci-GAL4* to drive *UAS-TT* and followed the GFP/RFP ratio in the domain of *ci* expression. Mid-third instar larvae with *ci-GAL4* driving the expression of *UAS-TT* showed comparatively uniform distributions of destabilized GFP and RFP throughout the whole anterior compartment, indicating stable expression of *ci* (Fig. 4A,C). In late-third instar larvae, the distribution shifts, with lower levels of destabilized GFP relative to RFP close to the compartment boundary where *en* expression is activated (Fig. 4B,D). This late shift reflects decreased *ci* expression along the compartment boundary where anterior *en* expression is activated.

Together, these results show that loss of anterior compartment expression of *en* both increases the expression of *ci* and of its target *ptc* and reduces the LV3-LV4 spacing. They suggest that the control of *ci* expression along the A/P boundary by the anterior Hh-dependent expression of *en* finely tunes the Hh gradient and/or transduction by controlling the levels of its receptor Ptc.

Overexpression of *rdx* or loss of *Su(fu)* impairs the ability of full-length Ci to compete with repressor-like Ci^{Ce2}

Next, we examined whether anterior compartment expression of *rdx* along the compartment boundary could also affect wing patterning and Hh signaling. A *UAS-RNAi* line targeting *rdx* was expressed in the anterior cells adjacent to the compartment boundary using *ptc-GAL4*. Similar to what was suggested with unmarked rdx^{5} wing clones (Kent et al., 2006), downregulation of *rdx* along the compartment boundary has little effect on the positioning of LV3 (compare Fig. 1D with Fig. 1A,B) or its primordium (Fig. S2A,B). Note that expression of this UAS-RNAi-*rdx* line was able to knock down *rdx* expression, as it suppressed the phenotype induced by overexpression of *UAS-rdx-myc* (Fig. S2C,D,E).

Previous studies in mouse have shown that the mammalian homologue of Rdx, SPOP, specifically targeted the full-length forms of Gli2 and Gli3 (Ci homologues) but not the Gli3 repressor, and that loss of Su(fu) destabilizes full-length Gli2 and Gli3 (Wang et al., 2010). Therefore, we examined whether Rdx affected the competition between the full-length Ci and a repressor-like form of Ci, and what role Su(fu) might have in modulating those effects. For this purpose we used the ci^{Ce2} mutation, which encodes a truncated Ci protein of 975 amino acids that mimics the Ci repressor as it is missing the CBP binding site for transactivation (Chen et al., 2000) and the C-terminal Su(fu) binding site (Croker et al., 2006; Han et al., 2015; Oh et al., 2015). In heterozygous flies, Ci^{Ce2} protein is

Development (2022) 149, dev200159. doi:10.1242/dev.200159

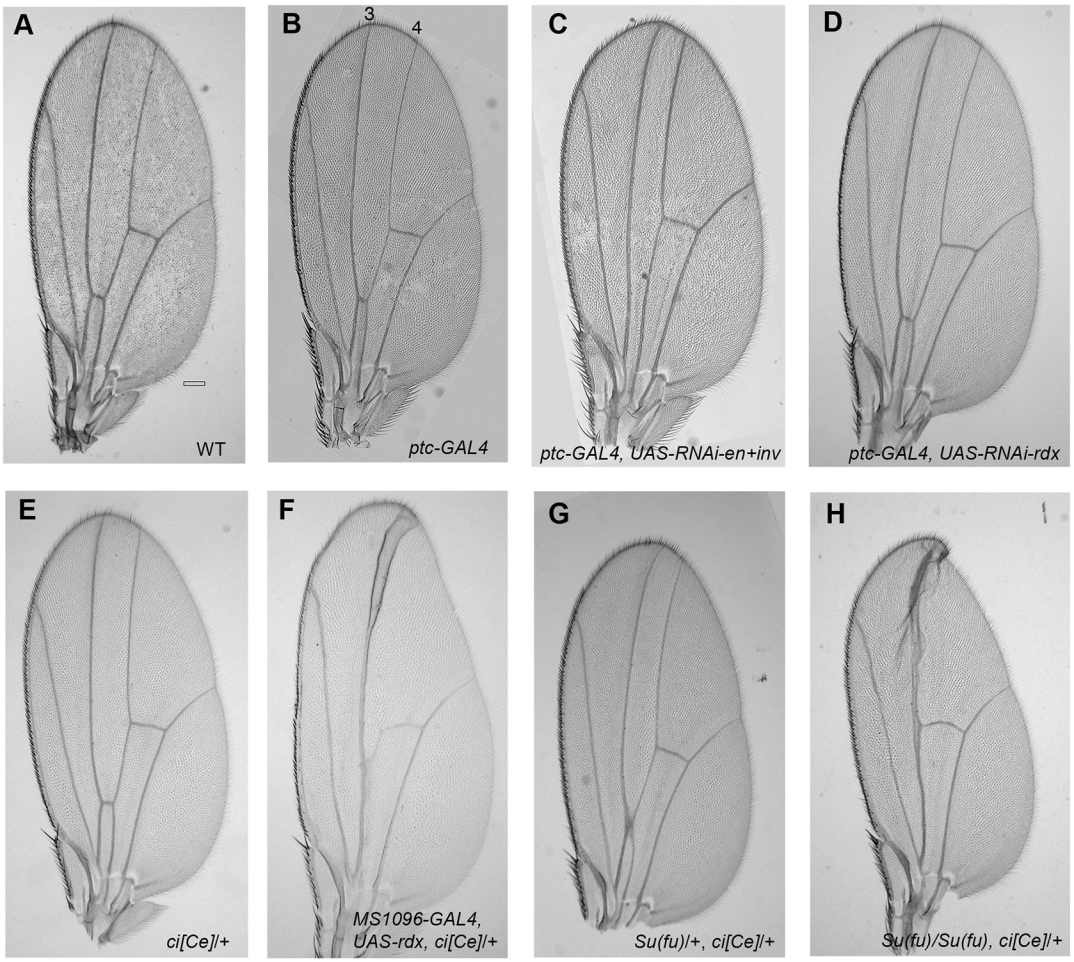

Fig. 1. The effects of manipulating the expression of *en*, *rdx*, *ci* and *Su(fu)* on *Drosophila* wing morphogenesis. (A) Wild-type wing. (B) In control *ptc-GAL4* (*ptc*$^{559.1}$)/+ flies, wing patterning is relatively normal, with a slight expansion in the domain between longitudinal vein (LV) 3 and LV4. (C) In flies in which the expression of *en* and *inv* has been knocked down specifically in the anterior compartment adjacent to the A/P compartment boundary [*w*; *ptc-GAL4* (*ptc*$^{559.1}$)/*UAS-RNAi-inv*(KK101934); *UAS-RNAi-en*(v35697)/+] the domain between LV3 and LV4 has been substantially reduced, decreasing from 0.226 mm^2±0.007 mm^2 (mean±s.d.) in *ptc-GAL4*/+ (*n*=10) to 0.151 mm^2±0.009 mm^2 in [*w*; *ptc-GAL4* (*ptc*$^{559.1}$)/*UAS-RNAi-inv* (KK101934); *UAS-RNAi-en* (v35697)/+]; *n*=10, *P*=3.6E-20 (unpaired two-tailed Student's *t*-test). (D) Downregulation of *rdx* immediately anterior to the A/P compartment boundary of the wing pouch [*w*; *ptc-GAL4* (*ptc*$^{559.1}$)/*UAS-RNAi-rdx*(v28798)] does not alter the distance between LV3 and LV4. (E) *ci*^{Ce2}/+ wing. (F) Overexpression of *rdx* throughout the wing pouch in a *ci*^{Ce2}/+ background (*w MS1096-GAL4*/+; *UAS-rdx*-myc /+; *ci*^{Ce2}/+) results in a fusion of LV3 and LV4. (G) In *Su(fu)*^{LP}/+; *ci*^{Ce2}/+ wings the distance between LV3 and LV4 is reduced. (H) In *Su(fu)*^{LP}; *ci*^{Ce2}/+ LV3 and LV4 are fused. The phenotypes were very consistent in all the flies of each genotype, with at least eight wings for each genotype mounted for microscopy. Male wings were used for the analysis with the exception of panel F. Anterior to the left. Scale bar: 100 µm.

present throughout the anterior compartment, including the domain of high-level Hh signaling where it can compete with full-length Ci. As a consequence, enhancers with perfect Ci binding sites, as in the reporter *4bs-lacZ* (Hepker et al., 1999), are silenced even in the domain of high Hh signaling adjacent to the compartment boundary (Fig. S3B). Nonetheless, *ci*^{Ce2}/+ mutants usually have normal wing patterning (compare Fig. 1E with Fig. 1A), but overexpression of *rdx* in the *ci*^{Ce2}/+ sensitized background leads to a phenocopy of a moderately strong reduction in Hh signaling with a complete fusion between LV3 and LV4 (Fig. 1F). This effect correlates with a dramatic decrease in the expression of Hh target genes, as can be seen with the expression *ptc-lacZ* when *rdx* is overexpressed in the dorsal compartment of *ci*^{Ce2}/+ wing discs (Fig. S4A).

An opposite effect on wing vein patterning is observed when *rdx* is overexpressed in a wild-type background, where it leads to a mild expansion of the domain between LV3 and LV4 (Fig. S2D). These opposite outcomes are presumably a consequence of competition between full-length Ci and the repressor-like Ci^{Ce2} in the *ci*^{Ce2} heterozygotes. Overexpression of *rdx* in a wild-type background results in a modest reduction of *ptc* (Kent et al., 2006; Zhang et al., 2006), allowing Hh to reach further into the anterior compartment, expanding the domain between LV3 and LV4 while also attenuating *dpp* expression, leading to a smaller wing and a decrease in the domains anterior to LV3 and posterior to LV4. In contrast, overexpression of Rdx in a *ci*^{Ce2}/+ background results in a dramatic decrease in Hh target gene expression, eliminating the domain between LV3 and LV4 (Fig. 1F, Fig. S4).

Because previous overexpression experiments had shown that Su(fu), which binds Ci, could partially protect it from Rdx-mediated degradation (Zhang et al., 2006), we examined whether there was a genetic interaction between *Su(fu)* and *ci*^{Ce2}. As seen in *ci*^{Ce2}/+, *Su(fu)* mutants have normal wings (Préat, 1992). In *Su(fu)*/+; *ci*^{Ce2}/+ animals, the distance between LV3 and LV4 is reduced and the wing veins fuse at the site of the anterior cross vein (Fig. 1G). In *Su(fu)*; *ci*^{Ce2}/+ animals, the wings are reduced and show a strong/

Development (2022) 149, dev200159. doi:10.1242/dev.200159

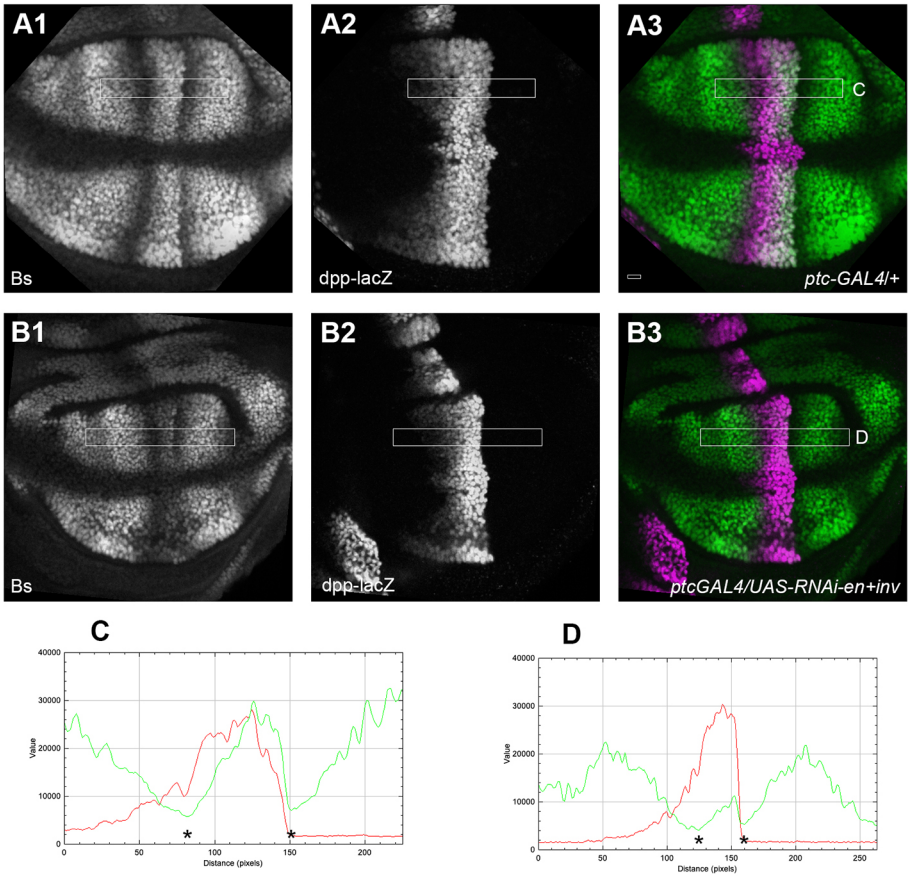

Fig. 2. Attenuation of *en* and *inv* expression in the anterior compartment narrows the stripes of Bs and *dpp* expression between LV3 and LV4. (A-D) Wing discs were double-labeled with anti-Bs to visualize cells destined to make the wing intervein region and anti-β-Galactosidase (anti-β-Gal) to visualize the domain of *dpp* expression, using a *dpp-lacZ* reporter. (A) *yw; dpp*^{10638} *(lacZ) ptc-GAL4* (*ptc*$^{559.1}$)/+ wing disc; *n*=20. A1 shows anti-Bs; A2 shows anti-β-Gal (*dpp-lacZ*); A3 shows a merged image (anti-Bs, green; anti-β-Gal, magenta). White box marks location for readings in graph C. (B) *yw*; *dpp*^{10638} *(lacZ) ptc-GAL4* (*ptc*$^{559.1}$)/*UAS-RNAi-inv*(KK101934); *UAS-RNAi-en*(v35697)/+ disc in which the domains of *dpp* expression and intervein cells between LV3 and LV4 are more narrow; *n*=21. B1 shows anti-Bs; B2 shows anti-β-Gal (*dpp-lacZ*); B3 shows a merged image (anti-Bs, green; anti-β-Gal, magenta). White box marks location for readings in graph D. The graphs in C and D, respectively, show the intensity of antibody staining to Bs (green line) and β-Gal (red line) across the control and *en+inv* knockdown wing discs. Note that in D the expression of *dpp-lacZ* is higher directly adjacent to the compartment boundary, and that the expression domain of *dpp-lacZ* is narrower, as is the spacing between the primordia for LV3 and LV4 (asterisks). Here, and in subsequent wing disc images, anterior is to the left and dorsal is up. Scale bar: 10 µm.

total fusion between LV3 and LV4 (Fig. 1H). These changes in wing patterning are also observed in the developing wing disc in *Su(fu)*/+; *ci*^{Ce2}/+ animals, where the LV3/4 intervein region is less distinct, and in *Su(fu)*; *ci*^{Ce2}/+ animals, where it is missing (Fig. S5).

To examine the effects of loss of *Su(fu)* on the competition between full-length Ci and Ci^{Ce2}, clones lacking *Su(fu)* were generated in a *ci*^{Ce2}/+ background. As can be seen in Fig. 5A-D, loss of *Su(fu)* in this genetic context leads to a dramatic reduction in the expression of both *ptc-lacZ* and *dpp-lacZ*. By contrast, loss-of-function *Su(fu)* clones in a wild-type background had little effect on the expression of these target genes (Fig. S6A,B).

In summary, these data reveal that overexpression of *rdx* or loss of *Su(fu)* interact genetically with *ci*^{Ce2} in a similar fashion, likely by shifting the competition between wild-type full-length Ci and the truncated Ci^{Ce2} protein in favor of Ci^{Ce2}.

In the absence of Rdx, Su(fu) is not required for full-length Ci to compete with Ci^{Ce2}

The similar effects of *Su(fu)* loss-of-function and *rdx* overexpression in *ci*^{Ce2} heterozygotes suggest that one role of Su(fu) is to protect full-length Ci from Rdx. To test this hypothesis, clones double mutant for *Su(fu)*^{LP} and *rdx*^{5} were generated in a *ci*^{Ce2}/+ background and the expression of *dpp-lacZ* assayed. As can be seen in Fig. 5E, clones double mutant for *Su(fu)* and *rdx* show little to no effect on *dpp* expression, which corresponds to the phenotype of *rdx* mutant clones. This contrasts with the strong effect of single mutant *Su(fu)* clones and shows that loss of *rdx* can suppress the effect of *Su(fu)* in a *ci*^{Ce2}/+ background. In conclusion, these results show that Su(fu) and Rdx can modulate the competition between the full-length and repressor forms of Ci.

Full-length Ci enters the nucleus in conjunction with Su(fu), whereas Ci^{Ce2} enters the nucleus on its own

Previous work has shown that there are both N-terminal and C-terminal domain binding sites for Su(fu) in the Ci protein (Croker et al., 2006; Han et al., 2015; Oh et al., 2015). We have also shown that full-length Ci brings Su(fu) with it into the nucleus and that the Ci repressor does not (Sisson et al., 2006). We decided to revisit this experiment and specifically compare the nuclear import of Su(fu) in relation to that of full-length Ci and Ci^{Ce2}.

To increase the levels of endogenous Ci in the region directly adjacent to the compartment boundary for better visualization, we downregulated *en* and *inv* along the compartment boundary. As full-length Ci contains both nuclear localization and nuclear export signals and shuttles in and out of the nucleus, it is necessary to block CRM1 (Emb)-mediated nuclear export with Leptomycin B (LMB) to observe nuclear accumulation of full-length Ci in response to Hh signaling. Under these conditions, full-length Ci accumulates in the nucleus, as expected, along with Su(fu) in the entire domain of Hh signaling, including the domain of high level Hh signaling directly adjacent to the compartment boundary (Fig. S7A). Away from the domain of Hh signaling where full-length Ci is cytoplasmic, but Ci repressor is nuclear, Su(fu) remains primarily cytoplasmic (Fig. S7A). In animals heterozygous for *ci*^{Ce2}, Ci and Su(fu) are nuclear in the domain of Hh signaling as both full-length Ci and Ci^{Ce2} enter the nucleus. However, away from the boundary, Ci^{Ce2} is still able to enter the nucleus in the absence of Hh, whereas Su(fu) remains cytoplasmic (Fig. S7B). This nuclear localization of Ci^{Ce2} away from Hh signaling is presumably due to failure of Cos2, which is known to normally retain Ci in the cytoplasm in the absence of Hh

Development (2022) 149, dev200159. doi:10.1242/dev.200159

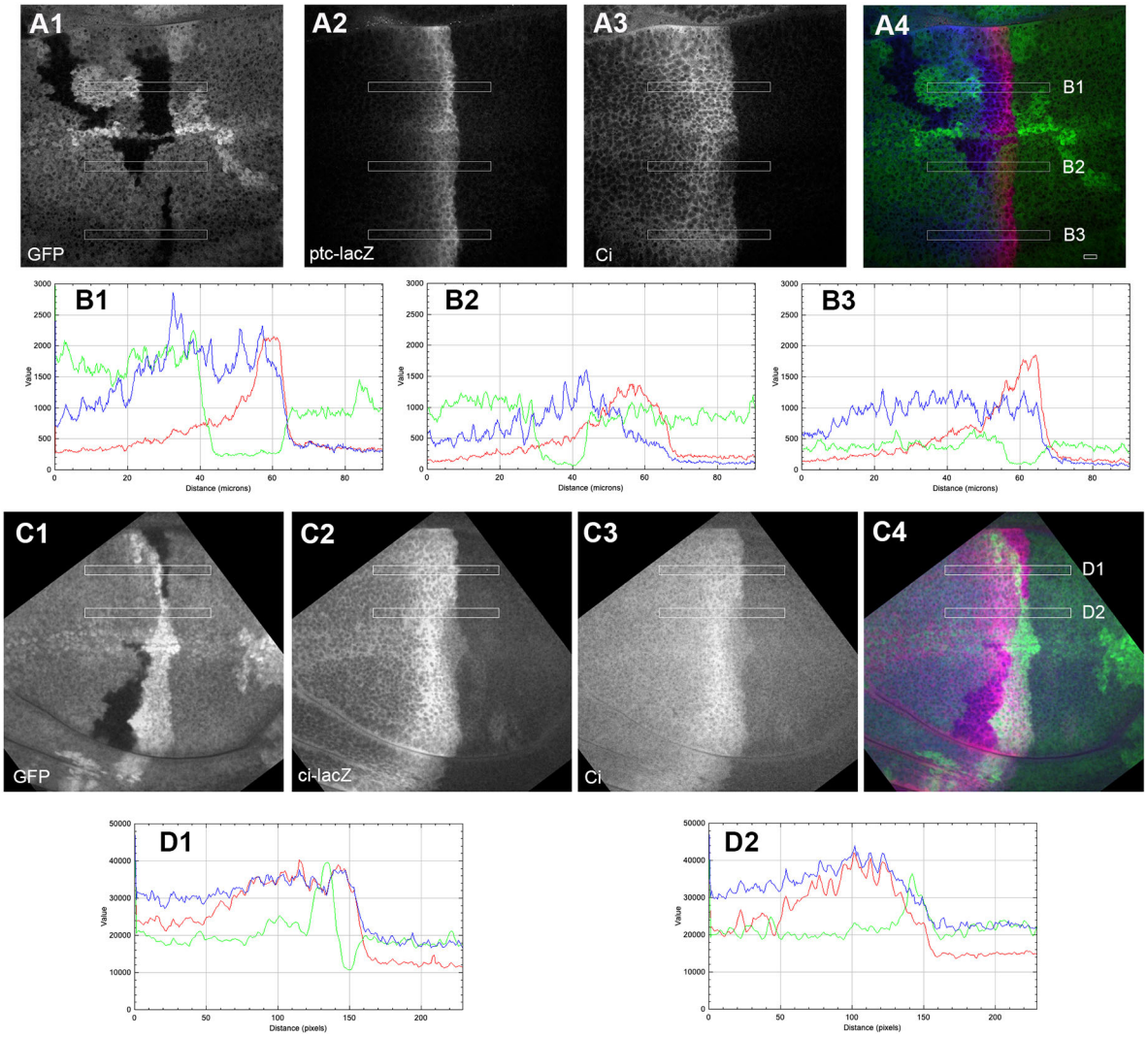

Fig. 3. Anterior clones mutant for *en* and *inv* show elevated expression of *ptc* and *ci*. (A) Wing imaginal discs of *yw hs-FLP*/+ or Y; *FRT42B en*^{E}/*FRT42B ubi-GFP*; *ptc-lacZ*/+. A1 shows clones mutant for *en*^{E} marked by the loss of GFP. A2 shows expression of *ptc* assayed by *ptc-lacZ*. A3 shows antibody staining to Ci. A4 shows a merged image of A1-A3 (GFP, green; β-Gal, red; Ci, blue); *n*=20. The bars labeled B1, B2 and B3 correspond to the three graphs below the figure. (B) Clones along the compartment boundary [marked by low levels of GFP (green line in bars B1 and B3)] have elevated levels of *ptc-lacZ* (red line) and Ci (blue line). (C) *yw hs-FLP*/+ or Y; *FRT42B en*^{E}/*FRT42B ubi-GFP*; *ci*^{Dplac}/+. C1 shows clones mutant for *en*^{E} marked by the loss of GFP. C2 shows expression of *ci* assayed by *ci*^{Dplac}. C3 shows antibody staining to Ci. C4 shows a merged image of C1-C3 (GFP, green; β-Gal, red; Ci, blue). The bars labeled D1 and D2 correspond to the two graphs below the figure. (D) Clones along the compartment boundary [marked by low levels of GFP (green line in bar D1)] have elevated levels of *ci-lacZ* (red line) and Ci (blue line); *n*=29. Scale bar: 10 µm.

(Chen et al., 1999; Wang and Holmgren, 2000), to sequester Ci^{Ce2} in the cytoplasm due to the absence of the C-terminal Cos2 binding site (called CORD) in Ci^{Ce2} (Wang and Jiang, 2004).

In summary, these results show that Su(fu) is in the nucleus with full-length Ci throughout the domain of Hh signaling, but not with Ci^{Ce2} nor presumably the repressor form. This raises the possibility that Su(fu) could protect full-length Ci, but not Ci^{Ce2}, nor presumably the repressor form, from Rdx.

Rdx helps to clear full-length Ci from the nucleus of cells no longer responding to Hh signaling

One example in which full-length Ci must be cleared from the nucleus is in the developing eye disc. With the passage of the morphogenetic furrow, cells must shut off *ci* for proper patterning (Lee and Treisman, 2002). Clearance of Ci posterior to the furrow is mediated by Cul3 (Ou et al., 2002) and Rdx (Kent et al., 2006; Zhang et al., 2006).

To examine whether a similar situation occurs in the wing disc, we again made use of the *UAS-TT* transcriptional timer (He et al., 2019), but in this case monitored the dynamics of *ptc* expression using *ptc*-GAL4. In comparison with the cells just along the compartment boundary, cells further away from the compartment boundary have a higher ratio of RFP relative to destabilized GFP, indicating that *ptc* expression is shutting off in these cells (Fig. 6A,C). This effect can be seen in individual cells at the anterior edge of the *ptc* expression stripe (Fig. 6E), where the boxed cell has a higher level of RFP expression versus a boxed cell abutting the compartment boundary that has higher levels of destabilized GFP (Fig. 6F). To assess the role of *rdx* in the dynamics of *ptc* downregulation away from the compartment boundary, *ptc-GAL4* was used to drive the expression of both *UAS-TT* and *UAS-RNAi-rdx*. Unlike the wild-type situation, RNAi knockdown of *rdx* leads to a more persistent expression of destabilized GFP in cells away from the compartment boundary (Fig. 6B,D).

Development (2022) 149, dev200159. doi:10.1242/dev.200159

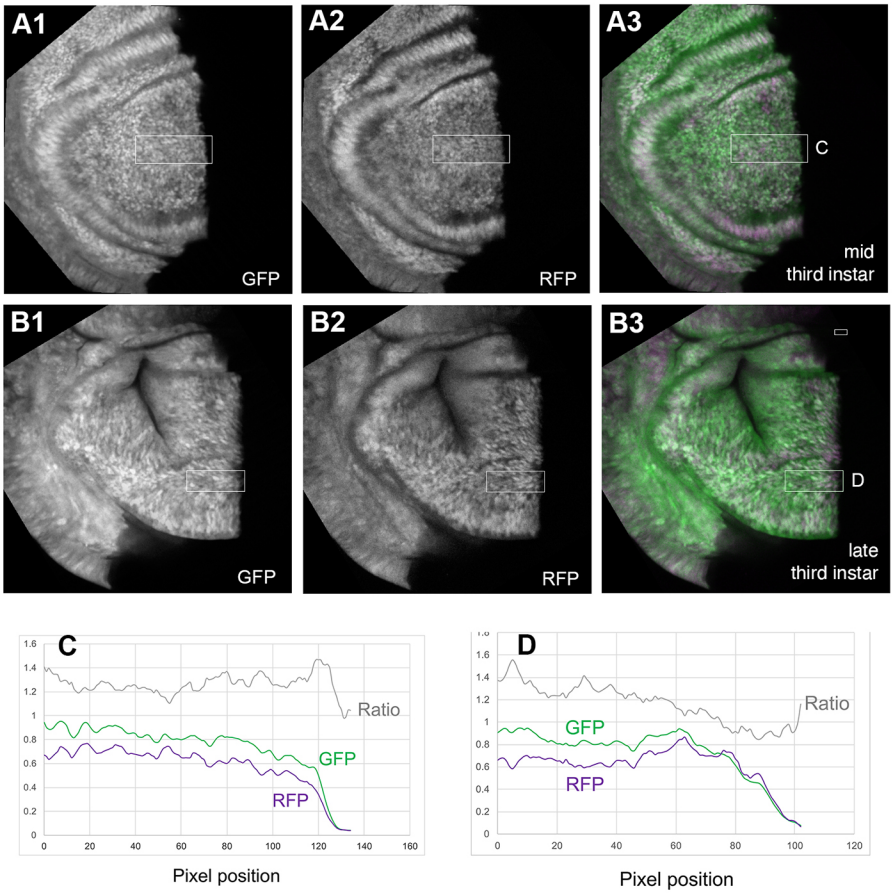

Fig. 4. *ci* expression is downregulated near the A/P compartment boundary in late-third instar larvae. (A) In mid-third instar larvae, *ci-GAL4* drives uniform expression of destabilized GFP and RFP from *UAS-TT* (*yw*; *ci-GAL4*/*UAS-TT*); *n*=7. A1 shows destabilized GFP. A2 shows RFP. A3 shows a merged image (GFP, green; RFP, magenta). (B) In late-third instar *yw*; *ci-GAL4*/*UAS-TT* larvae, the levels of destabilized GFP are lower along the compartment boundary relative to RFP; *n*=20. B1 shows destabilized GFP. B2 shows RFP. B3 shows a merged image (GFP, green; RFP, magenta). (C) Bar function of ImageJ used to graph the distribution of GFP, RFP and their ratio from panels in A. The *y*-axis is the ratio of GFP/RFP and fluorescence intensities in arbitrary units. (D) Bar function of ImageJ used to graph the distribution of GFP, RFP and their ratio from panels in B. The *y*-axis is the ratio of GFP/RFP and fluorescence intensities in arbitrary units. Scale bar: 10 µm.

DISCUSSION

In this study we examined the roles of three potential negative regulators of Hh signal transduction, two of which are themselves encoded by Hh target genes. In each case we discovered interesting new aspects about the pathway's regulation.

Anterior expression of *en* likely extends the range of the Hh gradient

Anterior expression of *en* in the wing imaginal disc was first observed 30 years ago and *en* is the Hh target gene requiring the highest level of Hh signaling. Its domain of expression exactly correlates with a region of lower full-length Ci protein levels. It had been proposed that the lower Ci protein levels are a consequence of Ci being particularly active and labile in this region (Ohlmeyer and Kalderon, 1998). We show here that the lower levels of Ci are not primarily due to it being particularly labile, but rather are a consequence of negative transcriptional regulation by En. The role of this negative feedback loop appears to be to modulate the Hh gradient by downregulating the expression of *ptc* in addition to its effects on *dpp* (Strigini and Cohen, 1997). This leads to Hh signaling extending further into the anterior compartment, with a corresponding anterior shift in the location of LV3 and the expression of *dpp*. We prefer a model in which the attenuation of *ptc* expression by anterior En is indirect via Ci (Fig. 7), but in principle En could also directly negatively regulate *ptc*. We feel this is less likely as, 'flip-out' clones expressing Ci activate high levels of *ptc* in the posterior compartment in the presence of En (Hepker et al., 1997). The anterior expression of *en* occurs late in third instar larvae (Blair, 1992), which correlates with the downregulation of *ci* expression as visualized using the *UAS-TT* transcriptional timer (Fig. 4B,D) and the refinement of wing vein specification (Blair, 2007).

Why did this mechanism evolve to modulate the Hh gradient? Morphogen gradients, by virtue of their central roles in the development of multiple tissues, must be robust and resistant to perturbation. Therefore, to specifically expand the range of the Hh gradient in the wing disc a new component was added, anterior expression of the *ci* repressor En.

Rdx and Su(fu) can modulate competition between the full-length and a repressor form of Ci

The lack of the C-terminal domain in the Ci repressor has multiple consequences. It loses the binding site for the co-activator CBP (Chen et al., 2000), and it loses C-terminal binding sites for Su(fu) (Croker et al., 2006; Han et al., 2015; Oh et al., 2015), Cos2 (Wang and Jiang, 2004) and Rdx (Zhang et al., 2009). As a consequence, the Ci repressor is not sequestered in the cytoplasm by Cos2 in the absence of Hh signaling and enters the nucleus without Su(fu), whereas full-length Ci enters the nucleus only in the presence of Hh signaling and as a complex with Su(fu).

In order to better understand the roles of Su(fu) and Rdx, we examined animals heterozygous for the ci^{Ce2} mutation. In this context, overexpression of *rdx* or loss of *Su(fu)* function leads to a complete fusion between LV3 and LV4. In addition, clones mutant for *Su(fu)* show dramatic reduction in the expression of the Hh target genes *ptc* and *dpp*. These results show that Su(fu) has a potential novel positive role in Hh signal transduction, improving the ability of full-length Ci to compete with the repressor form (Fig. 7). A positive role for Su(fu) has also been found in mammals where Su(fu) appears to function as a chaperone for the full-length

Development (2022) 149, dev200159. doi:10.1242/dev.200159

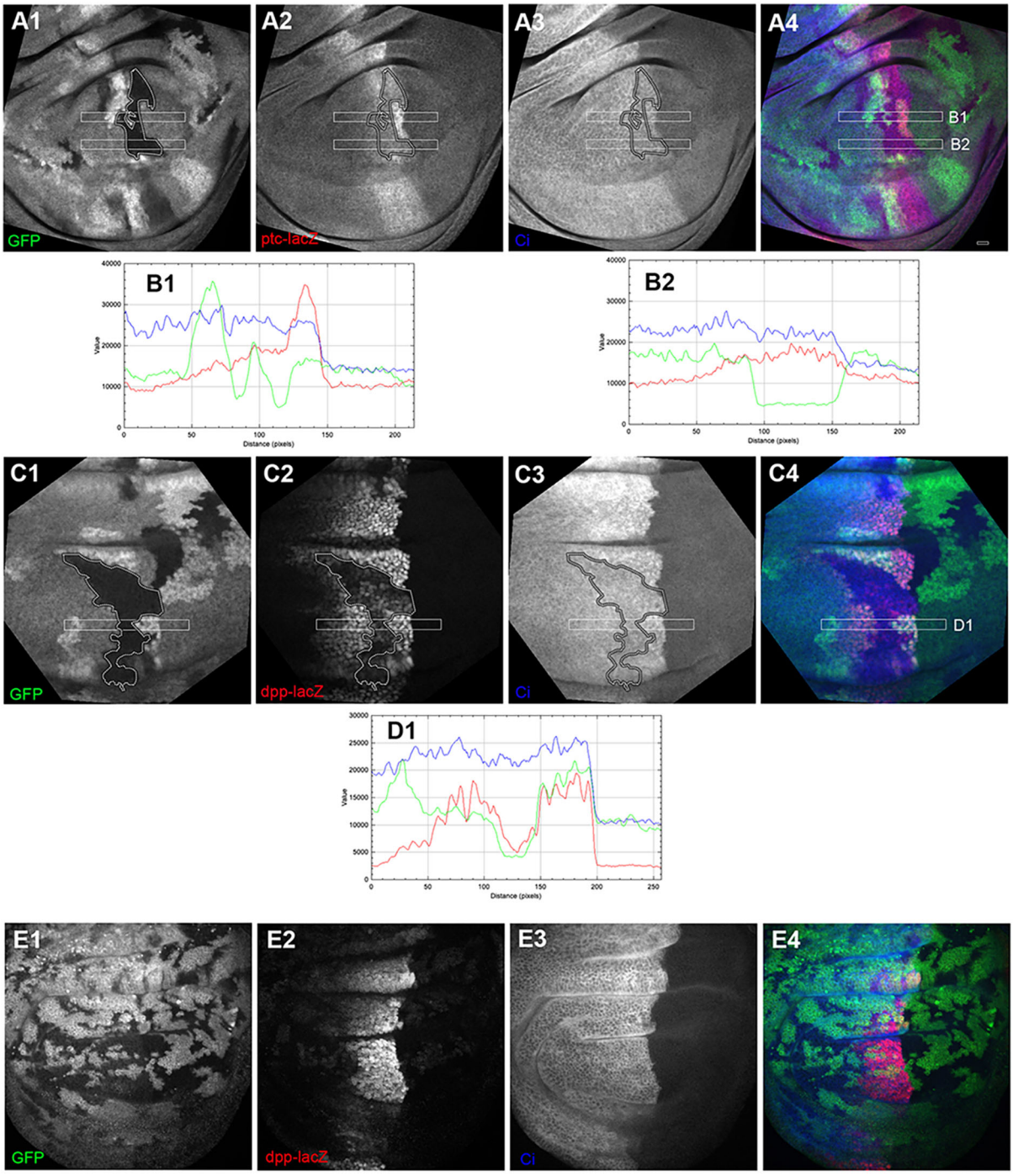

Fig. 5. Loss of *Su(fu)* decreases in the expression of *ptc* and *dpp* in a *ci*^{Ce2}/+ background and is dependent on *rdx*. (A) Clones mutant for *Su(fu)* in a *ci*^{Ce2}/+ background show a dramatic decrease in *ptc* expression [*yw hs-FLP*/+ or Y; *ptc-lacZ*/+; *FRT82B Su(fu)*^{LP}/*FRT82B ubi-GFP*; *ci*^{Ce2}/+]; anterior to the left. A clone along the compartment boundary is outlined in panels A1-A3. A1 shows *Su(fu)* mutant clones marked by the loss of GFP. A2 shows expression of *ptc-lacZ*. Note the significantly higher levels of *ptc* expression in the heterozygous *Su(fu)*^{LP} territory adjacent to the compartment boundary (see B1). A3 shows antibody staining of Ci. A4 shows a merged image of A1-A3 (GFP, green; β-Gal, red; Ci, blue); *n*=5. The bars labeled B1 and B2 correspond to the two graphs below the figure. (B) Adjacent to the compartment boundary anterior cells heterozygous for *Su(fu)* have high levels of *ptc* expression (GFP, green line; *ptc-lacZ*, red line; Ci, blue line) (B1). A clone along the compartment boundary [marked by low levels of GFP (green line in bar B2)] has low levels of *ptc-lacZ* (red line) (Ci, blue line). (C) Clones mutant for *Su(fu)* in a *ci*^{Ce2}/+ background show a dramatic decrease in *dpp* expression [*yw hs-FLP*/+ or Y; *dpp*^{10638} *(lacZ)*/+; *FRT82B Su(fu)*^{LP}/*FRT82B ubi-GFP*; *ci*^{Ce2}/+]; anterior to the left. A clone within the domain of *dpp* expression is outlined. C1 shows *Su(fu)* mutant clones marked by the loss of GFP. C2 shows expression of *dpp-lacZ*. C3 shows antibody staining of Ci. C4 shows a merged image of C1-C3 (GFP, green; β-Gal, red; Ci, blue); *n*=10. The bar labeled D1 correspond to the graph below the figure. (D1) A clone [marked by low levels of GFP (green line)] has decreased levels of *dpp-lacZ* (red line) (Ci, blue line). (E) Clones double mutant for *Su(fu)* and *rdx* in a *ci*^{Ce2}/+ background do not have a profound effect on the expression of *dpp* [*yw hs-FLP*/+ or Y; *dpp*^{10638} (*lacZ*)/+; *FRT82B Su(fu)*^{LP} *rdx*^{5}/*FRT82B M(3)w ubi-GFP*; *ci*^{Ce2}/+]. E1 shows *Su(fu) rdx* double mutant clones are marked by the loss of GFP. E2 shows that expression of *dpp-lacZ* is not significantly reduced in the clones. E3 shows antibody staining to Ci. E4 shows a merged image (GFP, green; β-Gal, red; Ci, blue); *n*=8. In order to recover *Su(fu)*^{LP} *rdx*^{5} mutant clones, it was necessary to use the Minute technique. Eggs were collected for 24 h, aged 6 days then heat shocked at 35°C for 1 h. Scale bar: 10 µm.

Development (2022) 149, dev200159. doi:10.1242/dev.200159

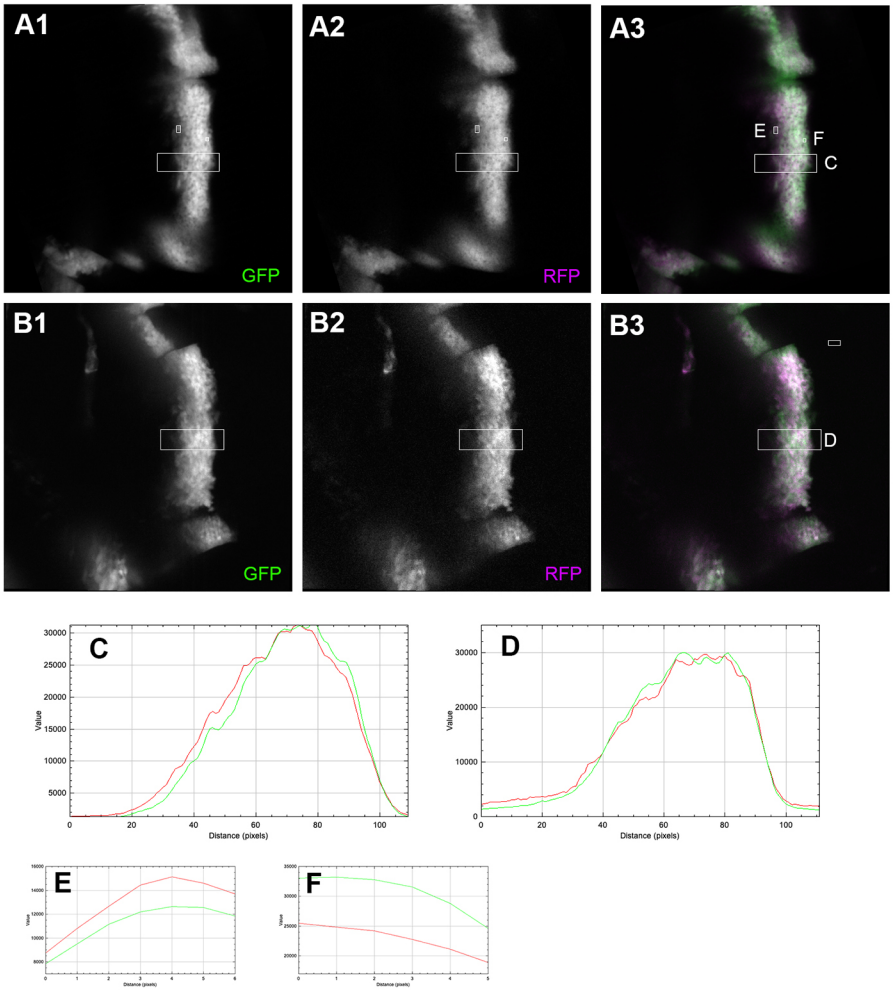

Fig. 6. Rdx facilitates the downregulation of *ptc* expression in cells away from the compartment boundary. (A) In *yw*; *ptc-GAL4*(*ptc*$^{559.1}$)/+; *UAS-TT*/+ animals, the levels of destabilized GFP are reduced relative to that of RFP in *ptc*-expressing cells away from the compartment boundary; *n*=15. A1 shows GFP fluorescence. A2 shows RFP fluorescence. A3 shows a merged image (RFP, magenta; GFP, green). (B) In *yw*; *ptc-GAL4*(*ptc*$^{559.1}$)/+; *UAS-TT, UAS-RNAi-rdx*(v28798)/+ animals the level of destabilized GFP is not reduced relative to RFP in *ptc*-expressing cells away from the boundary; *n*=13. B1 shows GFP fluorescence. B2 shows RFP fluorescence. B3 shows a merged image (RFP, magenta; GFP, green). The bars labeled C-F in A and B correspond to the graphs below the figure. (C) Bar function of ImageJ used to graph the distribution of GFP (green line) and RFP (red line) from panels in A. (D) Bar function of ImageJ used to graph the distribution of GFP and RFP from panels in B. (E) Boxed cell away from the compartment boundary in panel A has reduced levels of destabilized GFP relative to RFP. (F) Boxed cell adjacent to the compartment boundary in panel A has elevated levels of destabilized GFP relative to RFP. Scale bar: 10 µm.

Gli proteins, but not the repressor forms, and is required for full activation of Gli target genes (Oh et al., 2015; Zhang et al., 2017). The requirement for *Drosophila* Su(fu) is obviated in the absence of Rdx, suggesting that Rdx primarily targets full-length Ci and not Ci repressor, even though the repressor is not protected by Su(fu) (Fig. 7). These results are analogous to what is seen with the mammalian homologue of Rdx, SPOP, indicating that this mechanism has been conserved during evolution. SPOP is opposed by Su(fu) and degrades the full-length forms of the mammalian GLI2 and GLI3 but not the GLI3 repressor form (Wang et al., 2010). The competition between Rdx and Su(fu) appears to be rather finely balanced as either increasing the expression of *rdx* or reducing the expression of *Su(fu)* enhances the ability of Ci^{Ce2} to compete with full-length Ci. This function of protecting full-length Ci from Rdx presumably takes place in the nucleus, as this is where the Rdx protein primarily localizes (Zhang et al., 2006; Seong and Ishii, 2013; Liu et al., 2014).

However, the functional relevance of *rdx* being an Hh target gene has been unclear. Zygotic loss of *rdx* in the embryo has no visible effect on segmental patterning of the cuticle (Kent et al., 2006) and, unlike *en*, knockdown of *rdx* along the compartment boundary in the wing disc has little effect on wing patterning. Perhaps its role is to clear full-length Ci from cells that were once within the domain of Hh signaling and have moved outside the domain of Hh signaling. Perdurance of Rdx could target full-length Ci in the nucleus allowing the Ci repressor to shut off Hh target genes. This is the situation in the eye disc with the progression of the morphogenetic furrow. Cells that recently received high level Hh signaling and activated Ci must now downregulate Ci to allow proper differentiation of the ommatidia. Rdx appears to be important for this process, as loss of *rdx* leads to defects in the eye (Kent et al., 2006; Zhang et al., 2006). A similar situation may exist in other tissues. Looking at the temporal regulation of *ptc* expression with *UAS-TT*, cells removed from the compartment boundary in the wing disc have lower levels of destabilized GFP relative to RFP and appear to be in the process of shutting off *ptc*. This distinction is lost following downregulation of *rdx* by RNAi.

In the domain of modest level Hh signaling (in which *dpp* is expressed), both full-length Ci and Ci repressor must be present in some form of reciprocal gradients. In this domain, enhancers with perfect Ci consensus binding sites are silent due to binding of Ci repressor. The *dpp* enhancer with imperfect Ci binding sites is expressed, and for it to be completely active, full-length Ci must be bound (Müller and Basler, 2000). Why is full-length Ci able to better compete with Ci repressor for the imperfect binding sites? Full-length Ci and the Ci repressor share the same DNA binding domain, and it would be expected that the repressor would outcompete full-length Ci for binding to target sites because the repressor is primarily nuclear, whereas full-length Ci is primarily cytoplasmic, even in the presence of Hh signaling, due to a strong nuclear export signal (NES). In Parker et al., 2011, they suggest that

Development (2022) 149, dev200159. doi:10.1242/dev.200159

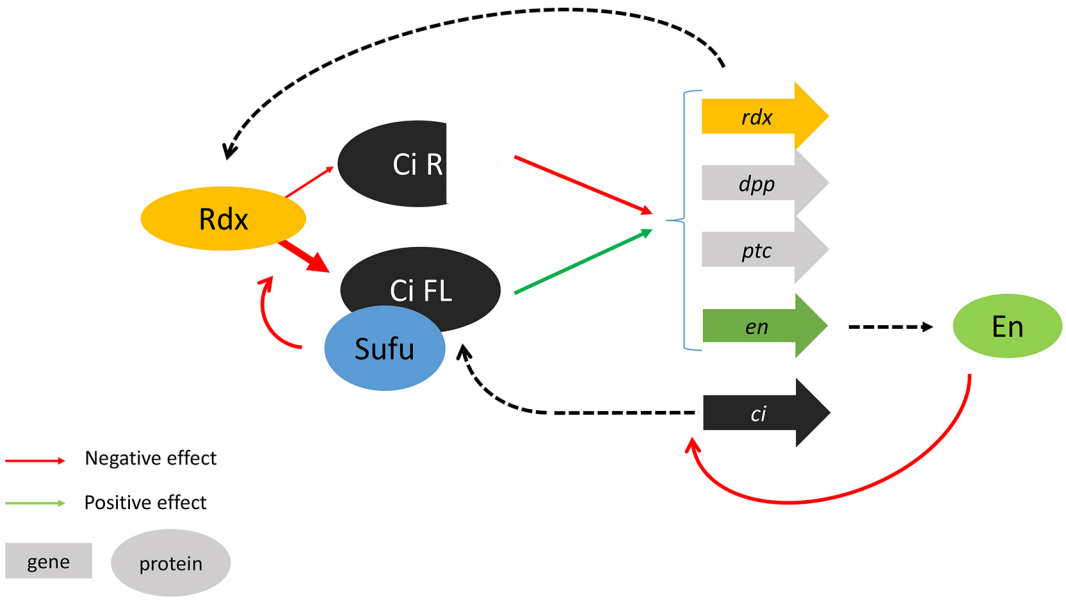

Fig. 7. Ci function is modulated by two feedback loops acting at different levels. Anterior expression of the En protein attenuates Ci activity directly adjacent to the compartment boundary of the wing disc by downregulating the expression of the *ci* gene. Rdx and Su(fu) act at the protein level modulating the competition between the full-length (Ci FL) and repressor forms (Ci R) of Ci. Rdx specifically targets full-length Ci, whereas Su(fu) partially protects full-length Ci from Rdx-mediated degradation. Rdx degradation of full-length Ci appears to help downregulate Hh target genes in cells no longer receiving the Hh signal.

cooperativity between Ci repressor proteins at perfect Ci binding sites can account for this distinction. Another potential mechanism for preferentially recruiting full-length Ci to imperfect binding sites might be suggested by the different protein interactions observed with full-length Ci and Ci^{Ce2}. Full-length Ci enters the nucleus with Su(fu) while the Ci repressor is not bound to Su(fu). In addition, the Ci repressor is missing the CBP binding site. As a consequence, full-length Ci could engage in protein-protein interactions with other transcription factors that are not available to the Ci repressor. This added affinity to other proteins within the enhanceosome could allow the preferential recruitment of full-length Ci to enhancers with imperfect Ci binding sites. Differential protein-protein interactions may also explain why full-length Ci is still able to activate *ptc-lacZ* expression along the compartment boundary in ci^{Ce2}/+ heterozygotes (Fig. S4) but not the artificial enhancer *4bs-lacZ* (Fig. S3). The *ptc-lacZ* enhancer is a bona fide *Drosophila* enhancer and is likely to recruit a constellation of proteins that could interact with full-length Ci, whereas protein-protein interactions are likely to be much less robust at *4bs*.

In conclusion, these results highlight the complexity of Hh signal transduction and its modulation. Expressing *en* in the anterior compartment of the wing pouch modulates the Hh gradient, whereas Su(fu) has a surprising positive role in the pathway, acting to partially protect full-length Ci from the E-3 ligase Rdx that Ci activates.

MATERIALS AND METHODS

Drosophila lines

Most of the *Drosophila* lines were obtained from the Bloomington *Drosophila* Stock Center. The RNAi lines to *en*, *inv* and *rdx* were obtained from the Vienna *Drosophila* Resource Center. en^{E} and ci^{Dplac} were obtained from T. Kornberg (Cardiovascular Research Insttiute, University of California San Francisco, CA, USA); *ptc-lacZ*, *UAS-rdx-myc*, *FRT82B* rdx^{5} *e*, and *FRT82B* $Su(fu)^{LP}$ rdx^{5} were obtained from J. Hooper (Department of Cell and Developmental Biology, University of Colorado Denver, CO, USA); and *UAS-TT* was obtained from N. Perrimon (Department of Genetics, Harvard Medical School, MA, USA). *4bs-lacZ* and *ci-GAL4* (Croker et al., 2006) were generated in our lab.

Antibodies

Mouse anti-GFP was obtained from Roche (1:750; 11 814 460 001); mouse anti-Blistered/DSRF was provided by S. Blair (Department of Integrative Biology, University of Wisconsin Madison, WI, USA) (1:750; 61385, Active Motif); mouse anti-Su(fu) (1:5; 25H3), mouse anti-Myc (1:10; 9E10), and mouse anti-En (1:10; 4D9) were obtained from the Developmental Studies Hybridoma Bank; and rat anti-Ci (2A1) (1:1000) (Motzny and Holmgren, 1995) and rabbit anti-β-Galactosidase (1:75,000) (Hepker et al., 1999) were generated in our laboratory. Note that the 2A1 anti-Ci antibody recognizes an epitope present in full-length Ci and Ci^{Ce2}, but that epitope is missing from the Ci repressor.

Wings

Adult flies were collected in ethanol and the wings dissected. After two washes in isopropyl alcohol, wings were mounted in a mixture of Canada balsam and methyl salicylate and incubated overnight at 65°C. Wings were imaged with a Nikon Optiphot using brightfield illumination.

Imaginal disc clones

Unless otherwise noted, eggs were collected for 24 h, allowed to develop for an additional 48 h and then heat shocked for 1 h at 35°C. Antibody stainings were performed as in Carroll and Whyte (1989) and image analysis was carried out using ImageJ. In order to recover *Su(fu) rdx* double mutant clones (Fig. 5E), it was necessary to give them a growth advantage (the Minute technique) by including a mutation [M(3)w] on the homologous chromosome arm that disrupts the gene encoding the S3 ribosomal protein.

Discs expressing *UAS-TT* were dissected in PBS, fixed on ice for 10 min in PBS+10% glycerol and 0.37% formaldehyde, rinsed in PBS+10% glycerol and mounted in Vectashield. Imaginal discs were imaged using either a Nikon Yokogawa spinning disk system or a Zeiss LSM 710 confocal microscope. Image analysis was carried out using ImageJ.

Acknowledgements

We thank Tom Kornberg, Joan Hooper, Seth Blair and Norbert Perrimon for *Drosophila* stocks and reagents, the Biological Imaging Facility at Northwestern University and the ImagoSeine core facility of Institut Jacques Monod, member of France-BioImaging (ANR-10-INBS-04) for access and support of microscopy. Stocks obtained from the Bloomington *Drosophila* Stock Center (NIH P40OD018537) were used in this study. Antibodies from the Developmental Studies Hybridoma Bank were developed under the auspices of the Eunice Kennedy Shriver

National Institute of Child Health and Human Development and maintained by the University of Iowa.

Competing interests
The authors declare no competing or financial interests.

Author contributions
Conceptualization: A.P., R.A.H.; Methodology: I.B., A.P., R.A.H.; Formal analysis: N.R., I.B., A.P., R.A.H.; Investigation: N.R., I.B., A.P., R.A.H.; Resources: A.P., R.A.H.; Writing - original draft: R.A.H.; Writing - review & editing: I.B., A.P., R.A.H.; Funding acquisition: A.P.

Funding
This work was supported by an undergraduate research grant from Northwestern University, the Centre national de la recherche scientifique, the Université de Paris and the Fondation ARC pour la Recherche sur le Cancer (grant 1112).

Peer review history
The peer review history is available online at https://journals.biologists.com/dev/article-lookup/doi/10.1242/dev.200159.

References
Abouchar, L., Petkova, M. D., Steinhardt, C. R. and Gregor, T. (2014). Fly wing vein patterns have spatial reproducibility of a single cell. *J. R Soc. Interface* **11**, 20140443. doi:10.1098/rsif.2014.0443

Alves, G., Limbourg-Bouchon, B., Tricoire, H., Brissard-Zahraoui, J., Lamour-Isnard, C. and Busson, D. (1998). Modulation of Hedgehog target gene expression by the Fused serine-threonine kinase in wing imaginal discs. *Mech. Dev.* **78**, 17-31. doi:10.1016/S0925-4773(98)00130-0

Aza-Blanc, P., Ramírez-Weber, F.-A., Laget, M.-P., Schwartz, C. and Kornberg, T. B. (1997). Proteolysis that is inhibited by hedgehog targets Cubitus interruptus protein to the nucleus and converts it to a repressor. *Cell* **89**, 1043-1053. doi:10.1016/S0092-8674(00)80292-5

Biehs, B., Sturtevant, M. A. and Bier, E. (1998). Boundaries in the Drosophila wing imaginal disc organize vein-specific genetic programs. *Development* **125**, 4245-4257. doi:10.1242/dev.125.21.4245

Blair, S. S. (1992). Engrailed expression in the anterior lineage compartment of the developing wing blade of Drosophila'. *Development* **115**, 21-33. doi:10.1242/dev.115.1.21

Blair, S. S. (2007). Wing vein patterning in Drosophila and the analysis of intercellular signaling. *Annu. Rev. Cell Dev. Biol.* **23**, 293-319. doi:10.1146/annurev.cellbio.23.090506.123606

Briscoe, J. and Thérond, P. P. (2013). The mechanisms of Hedgehog signalling and its roles in development and disease. *Nat. Rev. Mol. Cell Biol.* **14**, 416-429. doi:10.1038/nrm3598

Carroll, S. B. and Whyte, J. S. (1989). The role of the hairy gene during Drosophila morphogenesis: stripes in imaginal discs. *Genes Dev.* **3**, 905-916. doi:10.1101/gad.3.6.905

Chen, Y. and Jiang, J. (2013). Decoding the phosphorylation code in Hedgehog signal transduction. *Cell Res.* **23**, 186-200. doi:10.1038/cr.2013.10

Chen, Y. and Struhl, G. (1996). Dual roles for patched in sequestering and transducing Hedgehog. *Cell* **87**, 553-563. doi:10.1016/S0092-8674(00)81374-4

Chen, C.-H., von Kessler, D. P., Park, W., Wang, B., Ma, Y. and Beachy, P. A. (1999). Nuclear trafficking of Cubitus interruptus in the transcriptional regulation of Hedgehog target gene expression. *Cell* **98**, 305-316. doi:10.1016/S0092-8674(00)81960-1

Chen, Y., Goodman, R. H. and Smolik, S. M. (2000). Cubitus interruptus requires Drosophila CREB-binding protein to activate wingless expression in the Drosophila embryo. *Mol. Cell. Biol.* **20**, 1616-1625. doi:10.1128/MCB.20.5.1616-1625.2000

Claret, S., Sanial, M. and Plessis, A. (2007). Evidence for a novel feedback loop in the Hedgehog pathway involving Smoothened and Fused. *Curr. Biol.* **17**, 1326-1333. doi:10.1016/j.cub.2007.06.059

Croker, J. A., Ziegenhorn, S. L. and Holmgren, R. A. (2006). Regulation of the Drosophila transcription factor, Cubitus interruptus, by two conserved domains. *Dev. Biol.* **291**, 368-381. doi:10.1016/j.ydbio.2005.12.020

Giordano, C., Ruel, L., Poux, C. and Therond, P. (2018). Protein association changes in the Hedgehog signaling complex mediate differential signaling strength. *Development* **145**, dev166850. doi:10.1242/dev.166850

Han, Y., Shi, Q. and Jiang, J. (2015). Multisite interaction with Sufu regulates Ci/Gli activity through distinct mechanisms in Hh signal transduction. *Proc. Natl. Acad. Sci. USA* **112**, 6383-6388. doi:10.1073/pnas.1421628112

Han, Y., Wang, B., Cho, Y. S., Zhu, J., Wu, J., Chen, Y. and Jiang, J. (2019). Phosphorylation of Ci/Gli by fused family kinases promotes Hedgehog signaling. *Dev. Cell* **50**, 610-26.e4. doi:10.1016/j.devcel.2019.06.008

He, L., Binari, R., Huang, J., Falo-Sanjuan, J. and Perrimon, N. (2019). In vivo study of gene expression with an enhanced dual-color fluorescent transcriptional timer. *eLife* **8**, e46181. doi:10.7554/eLife.46181

Hepker, J., Wang, Q. T., Motzny, C. K., Holmgren, R. and Orenic, T. V. (1997). Drosophila cubitus interruptus forms a negative feedback loop with patched and regulates expression of Hedgehog target genes. *Development* **124**, 549-558. doi:10.1242/dev.124.2.549

Hepker, J., Blackman, R. K. and Holmgren, R. (1999). Cubitus interruptus is necessary but not sufficient for direct activation of a wing-specific decapentaplegic enhancer. *Development* **126**, 3669-3677. doi:10.1242/dev.126.16.3669

Kent, D., Bush, E. W. and Hooper, J. E. (2006). Roadkill attenuates Hedgehog responses through degradation of Cubitus interruptus. *Development* **133**, 2001-2010. doi:10.1242/dev.02370

Kinnebrew, M., Luchetti, G., Sircar, R., Frigui, S., Viti, L. V., Naito, T., Beckert, F., Saheki, Y., Siebold, C., Radhakrishnan, A. et al. (2021). Patched 1 reduces the accessibility of cholesterol in the outer leaflet of membranes. *eLife* **10**, e70504. doi:10.7554/eLife.70504

Lee, J. D. and Treisman, J. E. (2002). Regulators of the morphogenetic furrow. *Results Probl. Cell Differ.* **37**, 21-33. doi:10.1007/978-3-540-45398-7_3

Lee, R. T. H., Zhao, Z. and Ingham, P. W. (2016). Hedgehog signalling. *Development* **143**, 367-372. doi:10.1242/dev.120154

Lefers, M. A., Wang, Q. T. and Holmgren, R. A. (2001). Genetic dissection of the Drosophila Cubitus interruptus signaling complex. *Dev. Biol.* **236**, 411-420. doi:10.1006/dbio.2001.0345

Liu, C., Zhou, Z., Yao, X., Chen, P., Sun, M., Su, M., Chang, C., Yan, J., Jiang, J. and Zhang, Q. (2014). Hedgehog signaling downregulates suppressor of fused through the HIB/SPOP-Crn axis in Drosophila. *Cell Res.* **24**, 595-609. doi:10.1038/cr.2014.29

Motzny, C. K. and Holmgren, R. (1995). The Drosophila cubitus interruptus protein and its role in the wingless and hedgehog signal transduction pathways. *Mech. Dev.* **52**, 137-150. doi:10.1016/0925-4773(95)00397-J

Müller, B. and Basler, K. (2000). The repressor and activator forms of Cubitus interruptus control Hedgehog target genes through common generic gli-binding sites. *Development* **127**, 2999-3007. doi:10.1242/dev.127.14.2999

Oh, S., Kato, M., Zhang, C., Guo, Y. and Beachy, P. A. (2015). A comparison of Ci/Gli activity as regulated by Sufu in Drosophila and mammalian Hedgehog response. *PLoS ONE* **10**, e0135804. doi:10.1371/journal.pone.0135804

Ohlmeyer, J. T. and Kalderon, D. (1998). Hedgehog stimulates maturation of Cubitus interruptus into a labile transcriptional activator. *Nature* **396**, 749-753. doi:10.1038/25533

Ou, C.-Y., Lin, Y.-F., Chen, Y.-J. and Chien, C.-T. (2002). Distinct protein degradation mechanisms mediated by Cul1 and Cul3 controlling Ci stability in Drosophila eye development. *Genes Dev.* **16**, 2403-2414. doi:10.1101/gad.1011402

Parker, D. S., White, M. A., Ramos, A. I., Cohen, B. A. and Barolo, S. (2011). The cis-regulatory logic of Hedgehog gradient responses: key roles for gli binding affinity, competition, and cooperativity. *Sci. Signal.* **4**, ra38. doi:10.1126/scisignal.2002077

Préat, T. (1992). Characterization of Suppressor of fused, a complete suppressor of the fused segment polarity gene of Drosophila melanogaster. *Genetics* **132**, 725-736. doi:10.1093/genetics/132.3.725

Radhakrishnan, A., Rohatgi, R. and Siebold, C. (2020). Cholesterol access in cellular membranes controls Hedgehog signaling. *Nat. Chem. Biol.* **16**, 1303-1313. doi:10.1038/s41589-020-00678-2

Ranieri, N., Ruel, L., Gallet, A., Raisin, S. and Thérond, P. P. (2012). Distinct phosphorylations on kinesin costal-2 mediate differential hedgehog signaling strength. *Dev. Cell* **22**, 279-294. doi:10.1016/j.devcel.2011.12.002

Robbins, D. J., Nybakken, K. E., Kobayashi, R., Sisson, J. C., Bishop, J. M. and Thérond, P. P. (1997). Hedgehog elicits signal transduction by means of a large complex containing the kinesin-related protein costal2. *Cell* **90**, 225-234. doi:10.1016/S0092-8674(00)80331-1

Sanial, M., Bécam, I., Hofmann, L., Behague, J., Argüelles, C., Gourhand, V., Bruzzone, L., Holmgren, R. A. and Plessis, A. (2017). Dose-dependent transduction of Hedgehog relies on phosphorylation-based feedback between the G-protein-coupled receptor Smoothened and the kinase Fused. *Development* **144**, 1841-1850. doi:10.1242/dev.144782

Seong, K.-H. and Ishii, S. (2013). Su(fu) switches Rdx functions to fine-tune hedgehog signaling in the Drosophila wing disk. *Genes Cells* **18**, 66-78. doi:10.1111/gtc.12018

Seong, K.-H., Akimaru, H., Dai, P., Nomura, T., Okada, M. and Ishii, S. (2010). Inhibition of the nuclear import of cubitus interruptus by roadkill in the presence of strong hedgehog signal. *PLoS ONE* **5**, e15365. doi:10.1371/journal.pone.0015365

Sisson, J. C., Ho, K. S., Suyama, K. and Scott, M. P. (1997). Costal2, a novel kinesin-related protein in the Hedgehog signaling pathway. *Cell* **90**, 235-245. doi:10.1016/S0092-8674(00)80332-3

Sisson, B. E., Ziegenhorn, S. L. and Holmgren, R. A. (2006). Regulation of Ci and Su(fu) nuclear import in Drosophila. *Dev. Biol.* **294**, 258-270. doi:10.1016/j.ydbio.2006.02.050

Strigini, M. and Cohen, S. M. (1997). A Hedgehog activity gradient contributes to AP axial patterning of the Drosophila wing. *Development* **124**, 4697-4705. doi:10.1242/dev.124.22.4697

Strutt, D. I. and Mlodzik, M. (1997). Hedgehog is an indirect regulator of morphogenetic furrow progression in the Drosophila eye disc. *Development* **124**, 3233-3240. doi:10.1242/dev.124.17.3233

Tabata, T., Eaton, S. and Kornberg, T. B. (1992). The Drosophila hedgehog gene is expressed specifically in posterior compartment cells and is a target of engrailed regulation. *Genes Dev.* **6**, 2635-2645. doi:10.1101/gad.6.12b.2635

Taipale, J., Cooper, M. K., Maiti, T. and Beachy, P. A. (2002). Patched acts catalytically to suppress the activity of Smoothened. *Nature* **418**, 892-897. doi:10.1038/nature00989

Wang, Q. T. and Holmgren, R. A. (2000). Nuclear import of cubitus interruptus is regulated by hedgehog via a mechanism distinct from Ci stabilization and Ci activation. *Development* **127**, 3131-3139. doi:10.1242/dev.127.14.3131

Wang, G. and Jiang, J. (2004). Multiple Cos2/Ci interactions regulate Ci subcellular localization through microtubule dependent and independent mechanisms. *Dev. Biol.* **268**, 493-505. doi:10.1016/j.ydbio.2004.01.008

Wang, C., Pan, Y. and Wang, B. (2010). Suppressor of fused and Spop regulate the stability, processing and function of Gli2 and Gli3 full-length activators but not their repressors. *Development* **137**, 2001-2009. doi:10.1242/dev.052126

Zhang, Q., Zhang, L., Wang, B., Ou, C.-Y., Chien, C.-T. and Jiang, J. (2006). A hedgehog-induced BTB protein modulates hedgehog signaling by degrading Ci/Gli transcription factor. *Dev. Cell* **10**, 719-729. doi:10.1016/j.devcel.2006.05.004

Zhang, Q., Shi, Q., Chen, Y., Yue, T., Li, S., Wang, B. and Jiang, J. (2009). Multiple Ser/Thr-rich degrons mediate the degradation of Ci/Gli by the Cul3-HIB/SPOP E3 ubiquitin ligase. *Proc. Natl. Acad. Sci. USA* **106**, 21191-21196. doi:10.1073/pnas.0912008106

Zhang, Z., Shen, L., Law, K., Zhang, Z., Liu, X., Hua, H., Li, S., Huang, H., Yue, S., Hui, C.-C. et al. (2017). Suppressor of fused chaperones Gli proteins to generate transcriptional responses to sonic Hedgehog signaling. *Mol. Cell. Biol.* **37**, e00421-16. doi:10.1128/MCB.00421-16

Zhou, Q., Apionishev, S. and Kalderon, D. (2006). The contributions of protein kinase A and smoothened phosphorylation to hedgehog signal transduction in Drosophila melanogaster. *Genetics* **173**, 2049-2062. doi:10.1534/genetics.106.061036

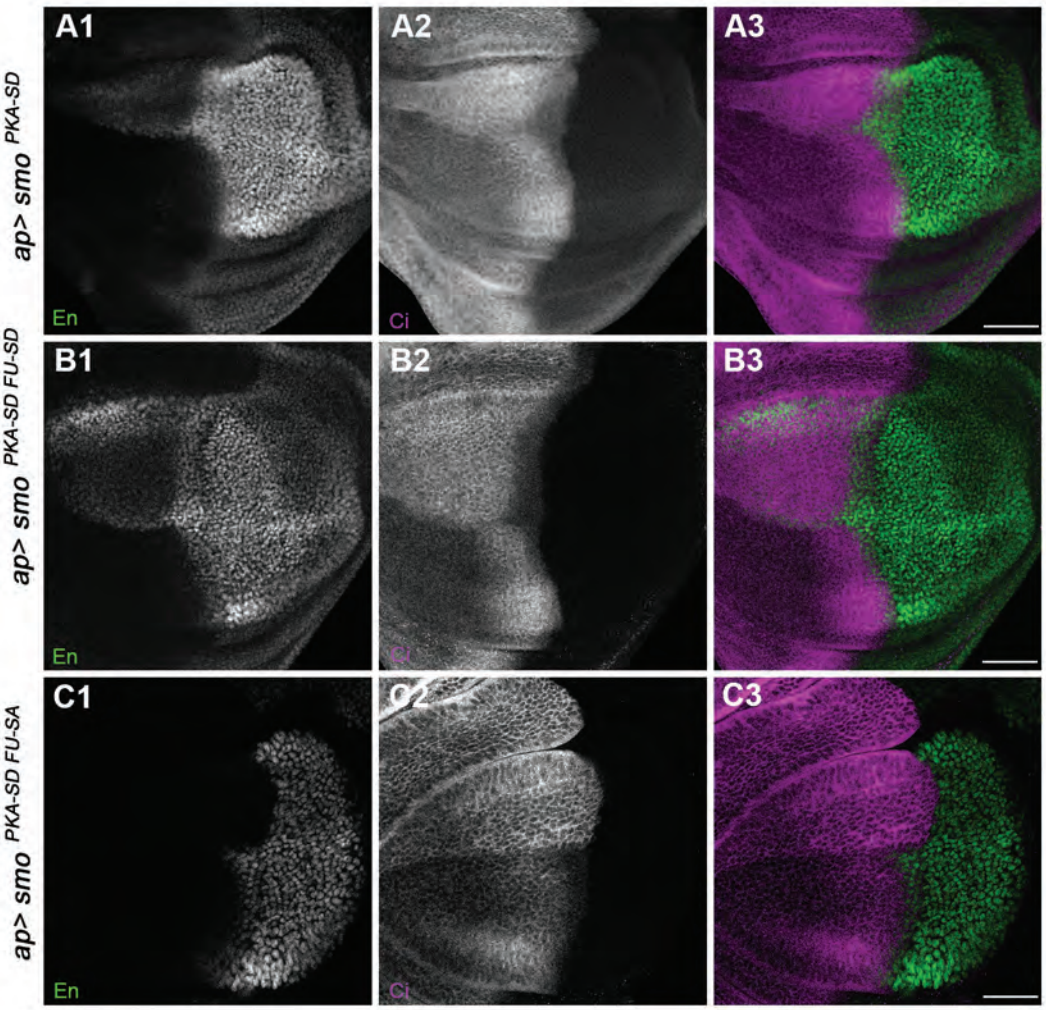

Fig. S1. Shifting the domain of anterior *en* expression causes a corresponding shift in the domain of low level Ci protein. Wing discs expressing activated Smo (*PKA-SD* and *PKA-SD FU-SD*) or attenuated Smo (*PKA-SD FU-SA*)(Sanial et al., 2017) in the dorsal compartment using *ap-GAL4*(ap^{md544}) and stained with antibodies against En (A1,B1,C1, green) and Ci (A2,B2,C2, magenta). Merge A3,B3,C3. (A) $UAS\text{-}smo^{PKA\text{-}SD}$, (B) $UAS\text{-}smo^{PKA\text{-}SD\ FU\text{-}SD}$ and (C) $UAS\text{-}smo^{PKA\text{-}SD\ FU\text{-}SA}$. The scale bars represent 50 um

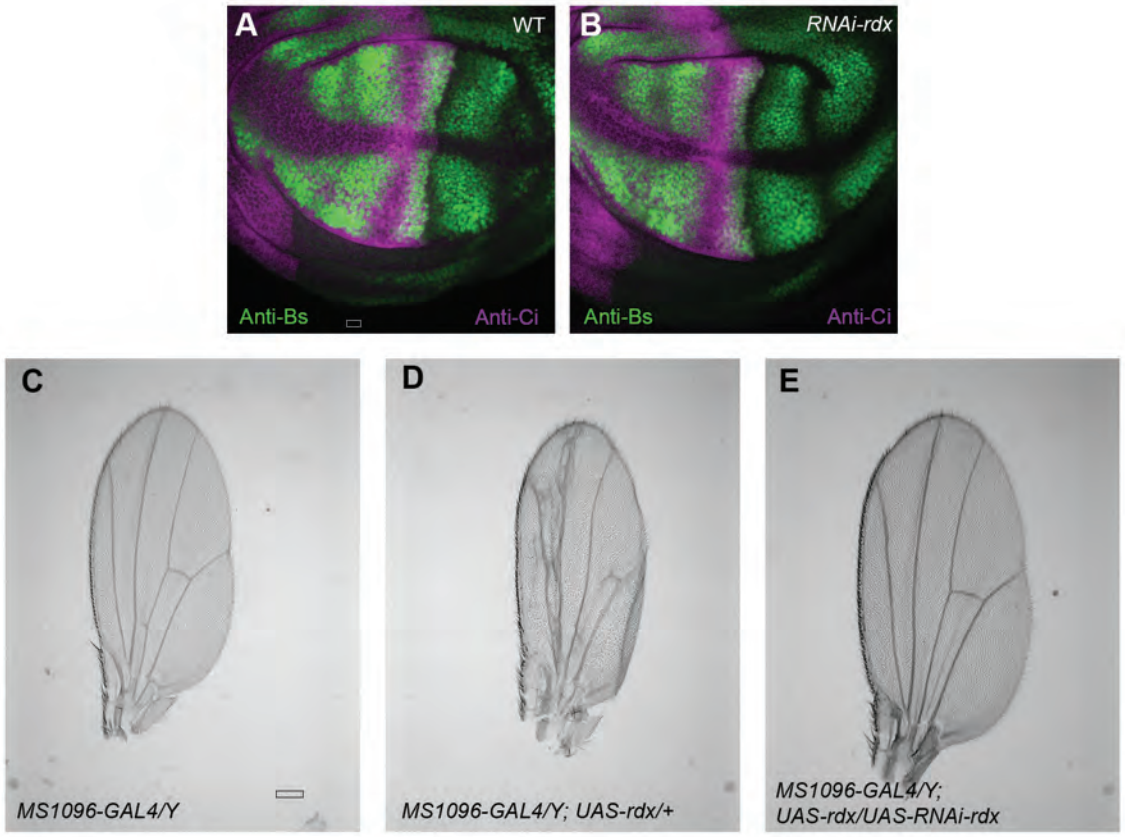

Fig. S2. RNAi targeting *rdx* does not significantly alter the position of the third wing vein primordium. (A and B) Wing discs were double labeled with anti-Bs (green) to visualize cells destined to make wing intervein and anti-Ci (magenta) to define the anterior compartment (anterior to the left). LV4 at the right edge of Ci expression marks the boundary between the anterior and posterior compartment. (A) Wild type wing disc n=6. (B) *yw*; *ptc-GAL4* (*ptc*$^{559.1}$)/*UAS-RNAi-rdx*(v28798)/+ n=4. Scale bar for panels A and B is in panel A and is 10 um. (C) Male fly wing hemizygous for *MS1096-GAL4*/Y. (D) *w MS1096-GAL4*/Y; *UAS-rdx-myc*/+. (E) *w MS1096-GAL4*/Y; *UAS-RNAi-rdx*(v28798), *UAS-rdx-myc*/+. The wing phenotypes were very consistent for each genotype and at least 10 wings were mounted for each genotype. Scale bar for panels C,D,E is in panel C and is 100 um.

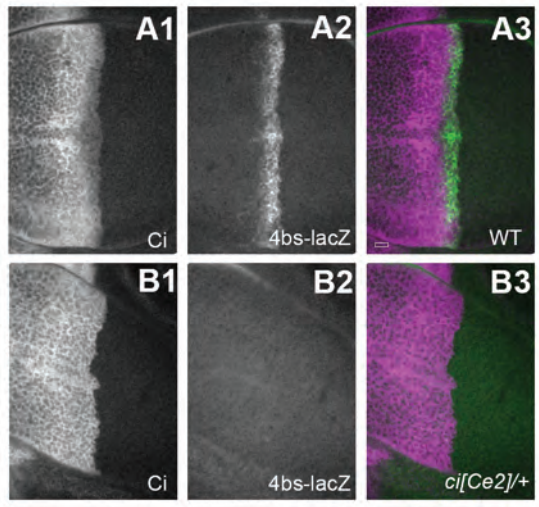

Fig. S3. Presence of a Ci repressor like protein along the compartment boundary prevents the expression of a reporter with perfect Ci binding sites. (A) Wild type animals show expression of *4bs-lacZ* (Hepker et al., 1999), a reporter construct with four perfect Ci binding sites (*4bs-lacZ*/+; ey^{D}/+), along the compartment boundary of the wing pouch (Anterior to the left). (A1) Antibody staining to Ci. (A2) *4bs-lacZ* expression along the compartment boundary. A3 is the merge of A1,2 (Anti-Ci magenta and anti--Gal green) n=4. (B) Animals heterozygous for the ci^{Ce2} mutation (*4bs-lacZ*/+; ci^{Ce2}/+) lose the expression of *4bs-lacZ* along the compartment boundary. (B1) Anti-Ci. (B2) Anti--Gal B3 is the merge of B1,2 (Anti-Ci magenta and anti--Gal green) n=6. In B1 note that there is no attenuation of Ci along the compartment boundary as there is in A1 due to the failure to express *en*. Scale bar for panels A and B is in panel A3 and is 10 um.

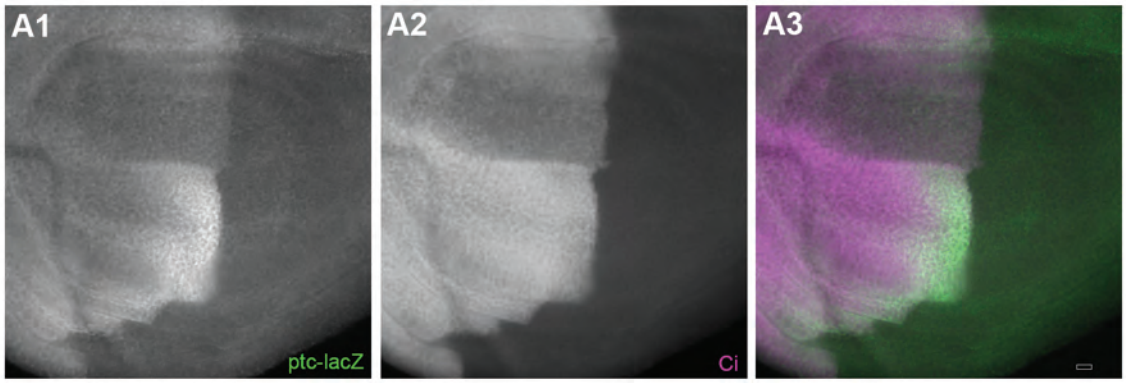

Fig. S4. Overexpression of *rdx* reduces Ci protein levels and the expression of *ptc-lacZ* in a *ci^{Ce2}*/+ background. Wing imaginal disc of the genotype *yw*; *ap-GAL4*(*ap^{md544}*)/*UAS-rdx-myc*; *ptc-lacZ*/+; *ci^{Ce2}*/+ in which *ap-GAL4* drives overexpression of *rdx* in the dorsal compartment (n=5). (anterior to the left, dorsal up) (A1) Anti--Gal visualization of *ptc-lacZ* shows dramatic attenuation of expression in the dorsal compartment. (A2) Anti-Ci. Ci levels are dramatically reduced in the dorsal compartment. (A3) Merge of A1 (anti--Gal green) and A2 (anti-Ci magenta). Scale bar in panel A3 and is 10 um.

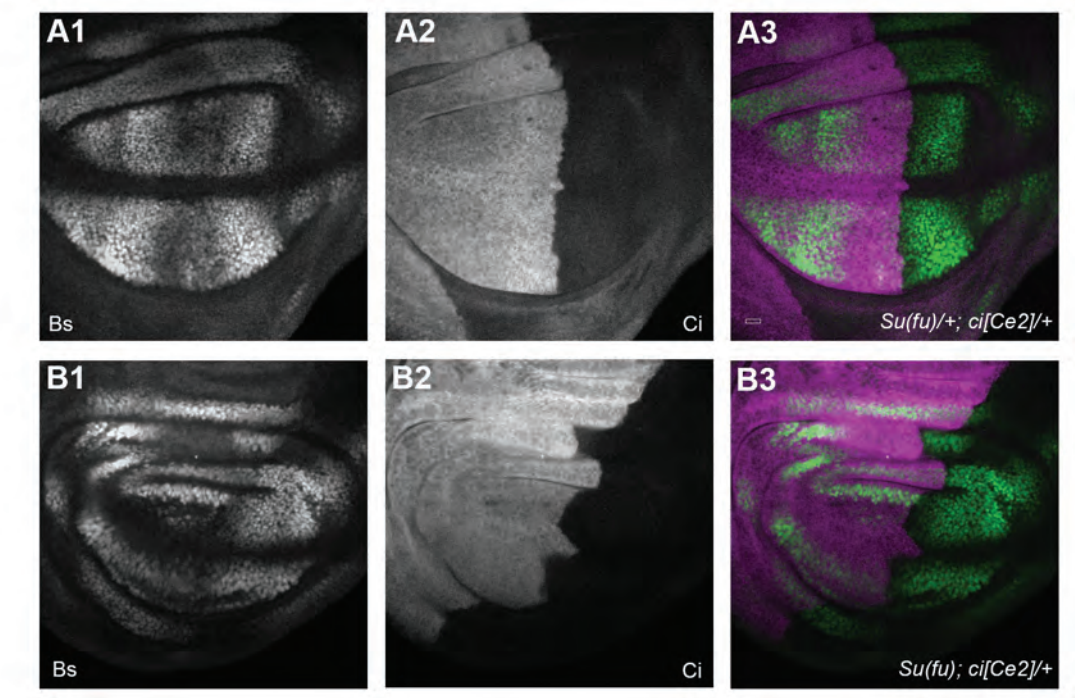

Fig. S5. ***Su(fu)*** **and** ***ci*^{Ce2}** **genetically interact and disrupt the patterning of the wing vein primordia.** (A) In *Su(fu)*^{LP}/+; *ci*^{Ce2}/+ wing discs, the 3/4 intervein region is not well defined as visualized using anti-Bs Antibody (A1). (A2) Anti Ci staining. (A3) merge Bs (green) Ci (magenta) n=4. (B) In *Su(fu)*^{LP}; *ci*^{Ce2}/+ wing discs, a single poorly defined wing vein primordium forms along the compartment boundary as visualized using anti-Bs Antibody (B1). (B2) Anti-Ci. (B3) merge Bs (green) Ci (magenta) n=5. Scale bar for panels A and B is in panel A3 and is 10 um.

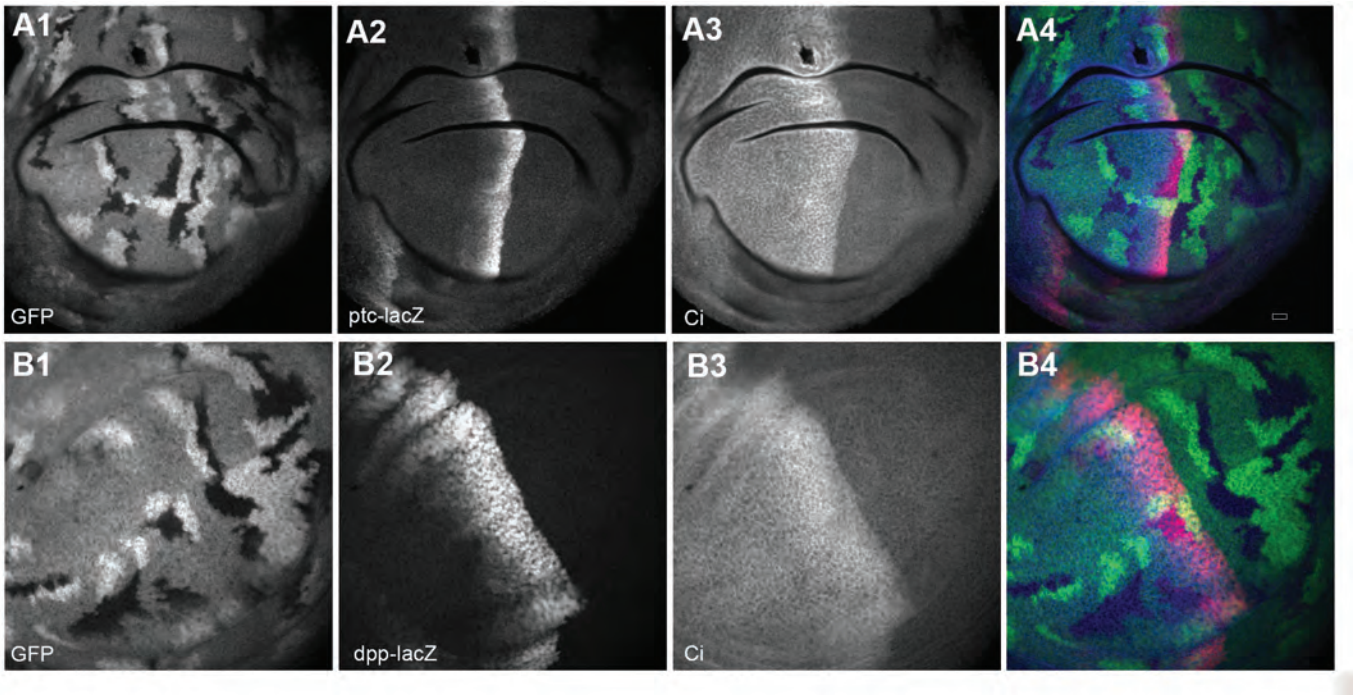

Fig. S6. On its own loss of *Su(fu)* has little effect on Hh target gene expression. (A) Clones mutant for *Su(fu)* do not have a profound effect on the expression of *ptc* in a wild type background (*yw hs-FLP*/+ or Y; *ptc-lacZ*/+; *FRT82B Su(fu)^{LP}/FRT82B ubi-GFP*; *ey^{D}*/+) (Anterior to the left). (A1) *Su(fu)* mutant clones marked by the loss of GFP. (A2) Expression of *ptc-lacZ*. (A3) Antibody staining of Ci. A4 is the merge of A1-3 (GFP in green, β-Gal in red, Ci in Blue) n=6. (B) Clones mutant for *Su(fu)* do not have a profound effect on the expression of *dpp* in a wild type background (*yw hs-FLP*/+ or Y; *dpp^{10638} (lacZ)*/+; *FRT82B Su(fu)^{LP}/FRT82B ubi-GFP*; *ey^{D}*/+) (Anterior to the lower left). (B1) *Su(fu)* mutant clones marked by the loss of GFP. (B2) Expression of *dpp-lacZ*. (B3) Antibody staining of Ci. B4 is the merge of B1-3 (GFP in green, βGal in red, Ci in Blue) n=8. Scale bar for panels A and B is in panel A4 and is 10 um.

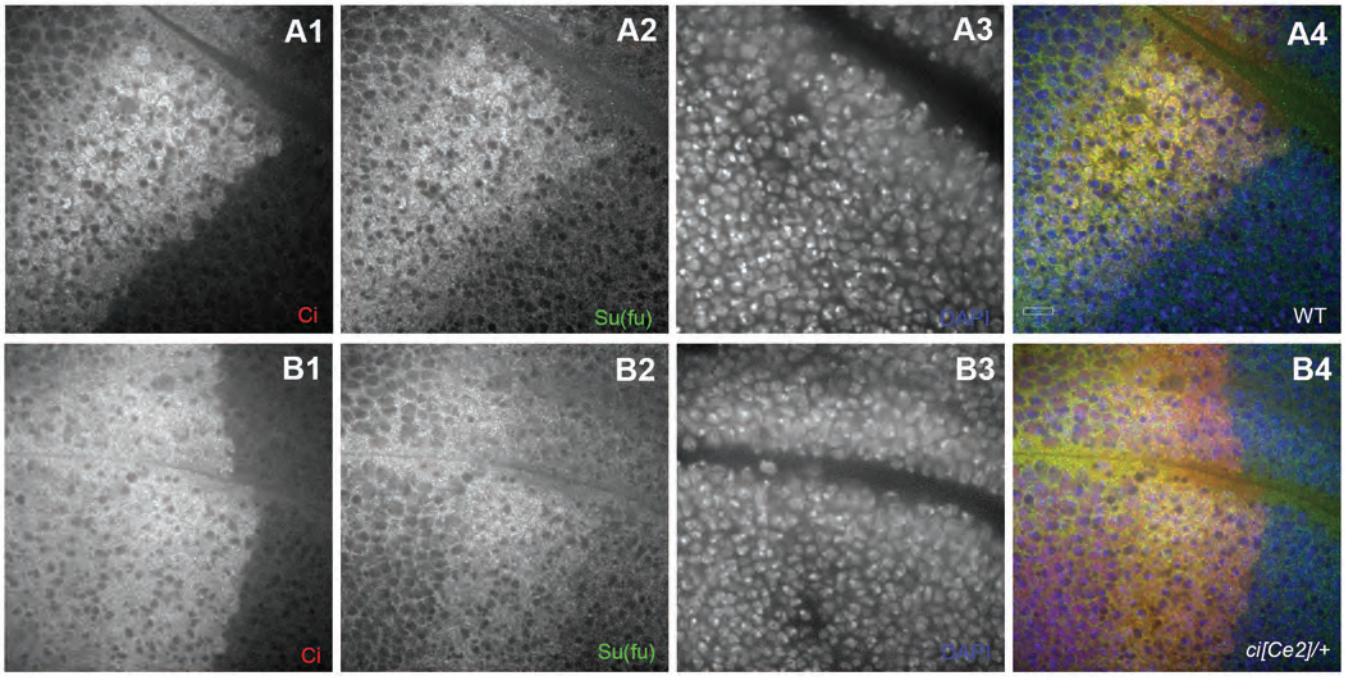

Fig. S7. In response to Hh signaling, full-length Ci accumulates in the nucleus with Su(fu) following treatment with the CRM1 inhibitor leptomycin B whereas Ci^{Ce2} accumulates in the nucleus without Su(fu). (A) *ptc-GAL4* (*ptc$^{559.1}$*)/ *UAS-RNAi-inv*(KK101934); *UAS-RNAi-en*(v35697)/+; *ey^{D}*/+ discs were treated with LMB for 1 hour (Anterior to the upper left). (A1) Antibody staining to Ci. In the domain of Hh signaling, Ci is present throughout the cell including the nucleus. Beyond the domain of Hh signaling Ci is cytoplasmic. (A2) As with Ci, Su(fu) is present throughout the cell in the domain of Hh signaling but is cytoplasmic anterior to the domain of Hh signaling. (A3) Nuclei stained with DAPI. A4 is the merge of A1-3 (Ci red, Su(fu) green, DAPI blue) n=5. (B) *ptc-GAL4* (*ptc$^{559.1}$*)/ *UAS-RNAi-inv*(KK101934); *UAS-RNAi-en*(v35697)/+; *ci^{Ce2}*/+ discs were treated with LMB for 1 hour (Anterior to the left). (B1) Antibody staining to Ci. Full-length Ci is throughout the cell in the domain of Hh signaling but cytoplasmic away from Hh signaling. Ci^{Ce2} is throughout the cell in the entire anterior compartment. (B2) Su(fu) is throughout the cell in the domain of Hh signaling, but away from Hh signaling where only Ci^{Ce2} accumulates in the nucleus, it is cytoplasmic. (B3) Nuclei stained with DAPI. B4 is the merge of B1-3(Ci red, Su(fu) green, DAPI blue) n=3. Scale bar for panels A and B is in panel A4 and is 10 um.